Available online at www.sciencedirect.com
SCIENCE DIRECT®
Composite Structures 63 (2004) 387–395
COMPOSITE STRUCTURES
www.elsevier.com/locate/compstruct

Numerical simulation of normal and oblique ballistic impact on ceramic composite armours

Z. Fawaz *, W. Zheng, K. Behdinan

Department of Aerospace Engineering, Ryerson University, 350 Victoria Street, Toronto, Ont., Canada M5B 2K3

Abstract

This paper presents three-dimensional finite element models that investigate the performance of ceramic–composite armours when subjected to normal and oblique impacts by 7.62 AP rounds. The finite element results are compared with experimental data from different sources both for normal and oblique impact, respectively. Simulation of the penetration processes as well as the evaluation of energy and stresses distributions within the impact zones highlight the difference between normal and oblique ballistic impact phenomena. The findings show that the distributions of global kinetic, internal and total energy versus time are similar for normal and oblique impact. However, the interlaminar stresses at the ceramic–composite interface and the forces at the projectile–ceramic interface for oblique impact are found to be smaller than those for normal impact. Finally, it is observed that the projectile erosion in oblique impact is slightly greater than that in normal impact.

Keywords: Ceramic; Composite; Finite element; Normal impact; Oblique impact; Ballistic impact; Lightweight armours

1. Introduction

Traditionally, armours have been made monolithic, usually of high hardness steel. However, the demands for lightweight armours for personal protection led to the investigation of alternative materials. In the last few decades, non-metallic materials, such as ceramics and composites, have been increasingly incorporated into more efficient lightweight armours. In particular, due to their low density, high hardness, high rigidity and strength in compression, ceramics have become widely used in armours. However, the low fracture toughness of ceramics and, consequently, their predisposition to fracture when subjected to high tensile stresses has led to the development of composite armours in which a ceramic-faced plate is backed by a more ductile material such as a metal or a polymeric composite that can resist failure due to tensile stresses. When armour-piercing projectiles impact onto composite armours, the projectiles are first shattered or blunted by the hard ceramic and the load is then spread over a larger area. The backing plate deforms to absorb the remaining kinetic energy of the projectile, delays the initiation of tensile failure in the ceramic and backing plate interface, and allows more projectile erosion. Since the pioneering work of Wilkins et al. [1], which was on the development of ceramic–aluminium armour systems, many research studies have been carried out to investigate the performance of composite armours. Accordingly, the use of ceramic-faced armours backed by a low-density metal or composite plate has become an accepted design approach for lightweight armours. Nevertheless, the performance of such multilayered armours under various ballistic impact scenarios has yet to be fully understood.

Lightweight armour design and analysis has been approached from all three analysis angles, namely: empirically, analytically, and numerically. Numerical models, based on solving all the governing equations over a spatial grid at successive time increments, have proven to be valuable design tools since they can help achieve a comprehensive understanding of the ballistic impact process. A number of numerical models simulating the ballistic impact process on two-component ceramic–metal and ceramic–composite armours have been published since the early 90s. Cortes et al. [2] proposed a model that was based on a finite difference Lagrangian formulation to simulate the normal impact on a ceramic target backed by a thin metallic plate without any front confinement. The macroscopic material behaviour in the zone of finely pulverized ceramic

* Corresponding author. Fax: +1-416-979-5308.
E-mail address: zfawaz@ryerson.ca (Z. Fawaz).

0263-8223/$ - see front matter © 2003 Published by Elsevier Ltd.
doi:10.1016/S0263-8223(03)00187-9

ahead of the penetrator was modelled by means of a constitutive relation taking into account internal friction and volumetric expansion. Their simulation predicted that once the ceramic is pulverized ahead of the projectile, the powder is pushed rather than penetrating. Wang et al. [3] implemented a ceramic model [4] in the explicit finite element code DYNA-2D and used the model to simulate their experiment on alumina ceramic–aluminium armour. They identified four different deformation mechanisms of the aluminium backing plate (petalling, plugging, partial penetration and indentation) as a function of backing plate thickness. Espinosa et al. [5] investigated the response of multilayered ceramic–steel targets to high velocity impact and penetration through finite element simulation. A multiple-plane microcracking model to describe the inelastic constitutive behaviour of ceramics in the presence of damage was integrated into the finite element code EPIC95. Their analyses showed that the penetration process is less dependent on the ceramic materials. By contrast, they found that the penetration process is highly dependent on the multilayered configuration and the target structural design (geometry and boundary condition). Zaera et al. [6] analysed the effect of the adhesive layer, used to bond ceramic tiles to a metallic plate, on the ballistic behaviour of ceramic–metal armours. In their study, numerical simulations were made of low calibre projectiles impacting on alumina tiles backed by an aluminium plate, using a commercial finite difference code AUTODYN-2D. Lee and Yoo [7] investigated numerically and experimentally the ballistic performance of ceramic–metal composite armour systems by varying the thickness of tiles, while maintaining equal areal density of the system. The cumulative damage model with smoothed particle hydrodynamics (SPH) scheme that had been implemented in to AUTODYN hydrocode was used in their simulation. The major features of composite armour system such as, projectile erosion, crack propagation, ceramic conoid formation and failure of backing plate were captured. Their simulation results of ballistic limit for selected targets revealed that there exists an optimum value of the front plate to back plate thickness ratio for a given areal density. The optimum thickness ratio of the front plate to back plate thickness for the configuration considered in their study was shown to be in the region of 2.5. Ceramic–composite armour systems were introduced in the 90s [8]. Chocron Benloulo and Sanchez-Galvez [9] developed a simple analytical model of high-velocity impact onto ceramic–composite armours. In order to verify the analytical model, they also numerically simulated the impact process by AUTODYN-2D commercial hydrocode. Sanchez-Galvez and Galvez Diaz-Rubio [10] performed numerical simulations of normal ballistic impact on ceramic–composite targets by using AUTODYN-2D hydrocode, where special subroutines for modelling the dynamic behaviour of ceramic and composite materials were implemented. The dynamic constitutive equations of ceramic that were proposed by Cortes et al. [11] were used in the simulation. Composites dynamic behaviour was modelled by assuming orthotropic elastic behaviour and the Tsai-Wu failure criterion.

Up to now, most of the numerical models that have been published on the subject of projectile perforation are limited to the case of normal impact on armours. Only a few analytical models on oblique ballistic impact on ceramic–metal armours have been published. Hetherington et al. [12,13] developed an analytical model for two-component composite armours subjected to an oblique impact. They observed that, circular contours of constant deformation which occur in backing plates under normal impact, tended to be elliptical for oblique impact. They assumed that the projectile tip deforms into an ellipse as it impacts the front face of the ceramic under the oblique impact. It was found that an inclined ceramic composite armour plate was more effective, on a thickness basis, than one arranged perpendicular to the line of impact; and the ballistic limit velocity increased with obliquity. Another analytical model for simulating ballistic impact on ceramic–metal armours has been proposed by Zaera and Sanchez-Galvez [14]. The model was based on Tata's [15] and Alekseevskii's [16] equation for projectile penetration into ceramic tile, whilst the response of metallic backing was modelled based on Woodward's [17] and den Reijer's [18] models. The mode was checked with date of residual mass and residual velocity of real fire tests of medium calibre projectiles on ceramic–metal armours.

In the current study, several sets of 3-D finite element models have been developed to investigate the response of a ceramic–composite integral armour system to normal and oblique penetrating projectiles. Comparison of the energy histories as well as stress and force distributions of armours subjected to normal and oblique impacts have been conducted by using the finite element code LS-DYNA3D.

2. Numerical models

2.1. Simulation tools

In the present study, the Hypermesh computer code has been used as the pre-processing tool. The numerical analysis of non-linear impact and penetration was performed using the non-linear finite element code LS-DYNA3D [19,20], which is dedicated to the analysis of dynamic problems associated with large deformation, low- and high-velocity impact, ballistic penetration and wave propagation, etc. As with all dynamics codes, LS-

Table 1
Material properties used in the finite element model

Material	ρ (kg/m^3)	E (GPa)	v	σ_y (Mpa)	E_t (GPa)	G (Gpa)
Steel	7890	202	0.3	1069	2.0	
Ceramic (AD-96)	3720	303	0.21	2108	0.0	
Composite	1600	80	0.3			25
Strength properties of the composite layer (Mpa) $X^C = 750$, $X^T = 1000$, $S = 250$						

DYNA3D seeks a solution to the momentum equation satisfying the traction and displacement boundary conditions on the exterior and interior boundaries respectively. The energy equation is integrated in time and is used for evaluating the equation of state and for a global energy balance. The integration scheme is based on the central difference method and the velocities and displacements are updated accordingly. The principal limitation during integration is the size of the time step, which should be small enough so that a second wave cannot travel across the smallest element during one integration step. The LSPOST computer code was used for post-processing.

2.2. Model development

A typical finite element model of ceramic–composite amour system consists of the normal and oblique impact of 60° conical–cylindrical steel projectiles on to ceramic–composite target. The steel projectile is 7.62 mm in diameter and 28.1 mm in length. Its performance is similar to that of a 7.62 mm NATO armour-piercing (AP) round. The target is AD96 alumina tile of 6.35 mm thickness supported by a high strength carbon/epoxy composite of 3.75 mm thickness. The thickness ratio is decided based on work by Hetherington [21] where it was concluded that the optimum thickness ratio of two-component composite armour was:

$$h_1/h_2 \approx 4(d_2/d_1) \quad (1)$$

where h_1 is ceramic plate thickness (mm), h_2 is backing plate thickness (mm), d_1 is the density of ceramic, and d_2 is density of backing plate. In this study, $d_1 = 3720$ kg/m^3, $d_2 = 1600$ kg/m^3 and therefore h_1 and h_2 are designed as 6.35 and 3.75 mm, respectively.

Two components, namely a ceramic plate and a composite plate, are used in the armour system. These two materials are defined with two material types of LS-DYNA. The ceramic is modelled with material type 3 (MAT_PLASTIC_KINEMATIC). This is a bi-linear elastic plastic model that contains formulations combining isotropic and kinematic hardening. Five material properties (Young's modulus E, Poisson's ratio v, Yield stress σ_y, tangent modulus E_t and hardening parameter β) are required for this material model, where E_t is the slope of the bi-linear stress strain curve. In the present analysis, hardening parameter is considered zero (kinematic hardening). The steel projectile is also modelled with material type 3 (MAT_PLASTIC_KINEMATIC). For the composite plate, material model type 59 (MAT_COMPOSITE_FAILURE_SOLID) is used. This is an orthotropic material model for solid element that uses a maximum stress failure criterion. Detailed descriptions of these material models can be found in LS-DYNA3D theoretical manual [20]. The corresponding material properties required for the models are taken from the literature and shown in Table 1.

Both plates composing the armour system are modelled with eight-noded uniform hexahedron solid elements whilst the projectile is modelled with six-noded tetrahedron solid elements. Due to the axisymmetric nature of the problem, only one half of the projectile-armour system is modelled in the present research. The nodes making up the projectile's mesh were assigned an initial velocity. The coordinate system and original mesh for normal impact is shown in Fig. 1.

The CONTACT_TIED_SURFACE_TO_SURFACE element was used to connect the ceramic and composite layers. This element allows the application of two failure criteria, namely a maximum normal tensile stress criterion and a maximum shear stress criterion. The interface between the projectile and armour material is defined with CONTACT_ERODING_SURFACE_TO_SURFACE. Projectile erosion is one of the major features of an armour penetration process. An erosion algorithm is

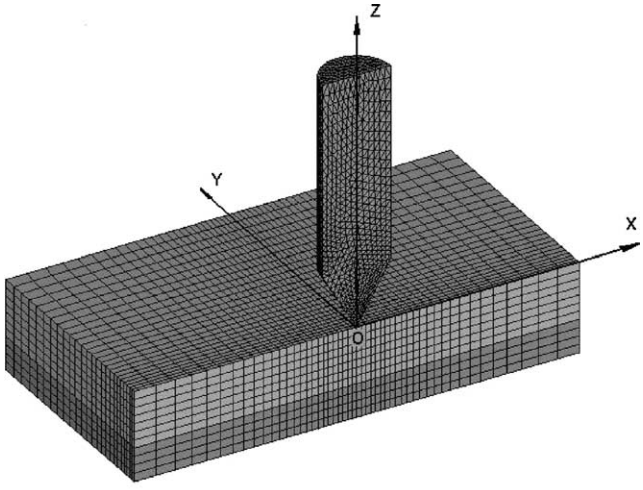

Fig. 1. Finite element model and coordinates for normal impact.

available in LS-DYNA3D code, which allows for penetration and perforation by eroding elements from the projectile surface as well as the target structure. The erosion is modelled based on the criterion that elements do not contribute to the physics of penetration if their effective plastic strain reaches a critical value (which is defined as erosion strain in LS-DYNA3D). If an element shares nodes at the surface and satisfies the criterion, then the stresses in it are brought to zero and the element is eroded away or eliminated from the grid. Upon erosion, the sliding interface between the projectile and the target is re-defined dynamically due to total element failure. In other words, computation can be carried out without the need for re-zoning distorted regions of the mesh during the penetration process.

2.3. Verification of the models

The numerical models were correlated with experimental data reported by Mayseless et al. [22] and Sadanandan and Hetherington [13] for normal and oblique impact, respectively. The material types and sizes as well as the conditions used in the computational models were the same as those reported in the aforementioned experimental studies. Material properties employed in the analysis were gleaned from the literatures. The steel and aluminium plates used in the ceramic–metal composite armours considered were modelled with material type 3 (MAT_PLASTIC_KINEMATIC) of LS-DYNA.

The experimental results obtained by Mayseless et al. [22] have been quoted in several publications [17,23]. Fig. 2 shows the comparison of ballistic limit and projectile erosion calculated using the present models with the experimental data reported in the aforementioned study. The ballistic limits thus calculated were found to be in reasonable agreement with the experimental results. The form of the curve depicting the erosion as a function of the initial velocity is correct, however, the actual size of erosion is overestimated by about 1–2 mm. The preliminary computations of oblique impact by 7.62 mm AP rounds on ceramic–aluminium targets were carried out to investigate the influence of oblique angle on ballistic limit. The calculations were compared with experimental results of Sadanandan and Hetherington [13] in Fig. 3, and the fit of computations to experimental data could be considered reasonable.

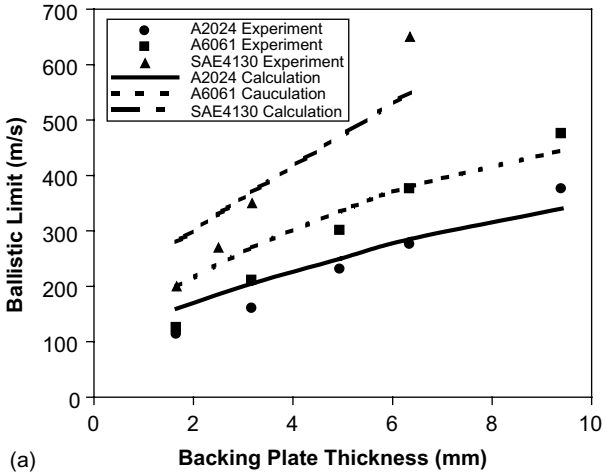

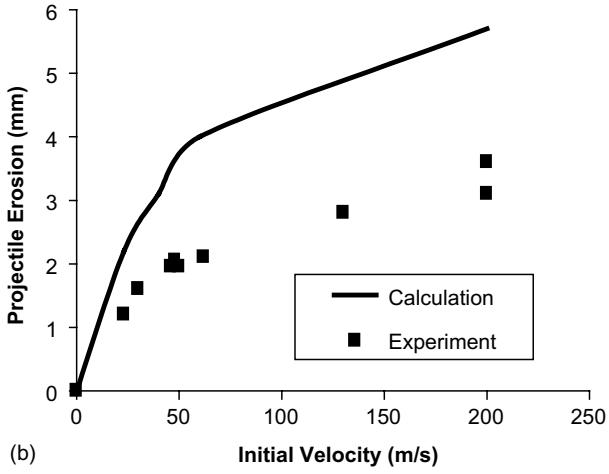

Fig. 2. Comparison between the experimental results for ballistic limit and projectile erosion and the results of the numerical model presented herein. (a) Ballistic limit and (b) projectile erosion.

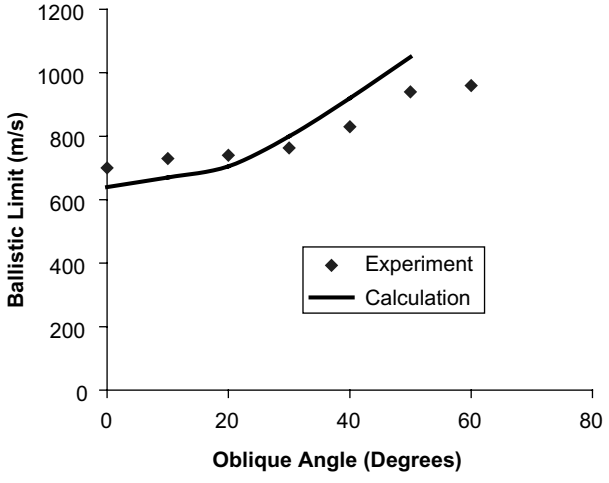

Fig. 3. Comparison of the ballistic limit computation with the experimental data of for oblique impact.

3. Results and discussion

Simulations of normal and 30° oblique impacts were performed, and some computation results are presented and discussed in this section. Initial velocities for both normal and oblique impact are 315 m/s. Solutions are terminated after 140 μs. The units for all calculations are

grams for mass, millimeters for length and microseconds for time.

After impact, the kinetic energy of the projectile is transferred to the armour, and as the projectile penetrates the armour, the kinetic energy will be reduced while the internal energy of the system will increase. Distributions of global kinetic, internal and total energy with respect to time are shown in Fig. 4. It should be noted that only one half of the system energy is represented in Fig. 4 because only one half of the spatial domain is considered. In spite of the difference between the normal impact process and the oblique one, their distributions of global energy are quite similar. It is observed that, for both normal and oblique impacts, the kinetic energy reduces at a faster pace than the rate at which the internal energy increases. This causes the total energy to decrease with the decrease of kinetic energy. The internal energy increases until around 50 μs and the kinetic energy decreases to zero within 70–80 μs. For oblique impact, the reduction of kinetic and total energy is about 10–20 μs slower than that for normal impact. Accordingly, the total energy decreases within 80–100 μs, and then stays at the same magnitude. The kinetic energy is computed by summation of $\left[\frac{1}{2} * \text{nodal mass} * \text{nodal velocity}^2\right]$ for all the nodes of the projectile and the target. The node-velocity term includes the x, y, and z components of the velocity. The kinetic energy dissipation is the result of the slowing down of projectile's velocity as well as the mass erosion of the projectile and target as the projectile ploughs through the armour. The kinetic energy reduces to zero when the node-velocity reduces to zero and the projectile comes to a complete stop. While the total energy in any physical system is conserved, the reduction in the total energy shown in Fig. 4 is due to the mass erosion of the system.

Fig. 5 depicts the projectile penetration processes in a ceramic–composite armour system for normal impact (Fig. 5(a)) and oblique impact (Fig. 5(b)). Once a projectile impacts the armour, fractures initiate immediately in the ceramic plate in a region near the projectile periphery. These fractures occur within 2 μs of initial contact and are attributed to the highly compressive stress in that region. Fig. 5(a) shows that for normal impact, at $t = 50$ μs, a conical region of crushed ceramic is found directly in front of the projectile and the fractures reach the ceramic–composite interface. The tip of the projectile reaches the end of the ceramic layer at $t = 60$ μs, then the projectile perforates the ceramic–composite interface and stop in the composite layer with 7.5 mm penetration at $t = 80$ μs. During the penetration process, the projectile is squashed and undergoes large lateral expansion. At the same time, the tip of the projectile is eroded. In this study, the total reduction in length of the projectile was found to be 6.54 mm (2.86 mm squashed and 3.68 mm eroded). When the projectile impacts the armour at 30° angle of obliquity with the same initial velocity as the normal impact, it cannot perforate the ceramic layer. Instead, the projectile is trapped within the ceramic layer at $t = 90$ μs, where it also ricochets slightly. In this case, the total penetration depth of the projectile is 4.54 mm and the cavity that formed during the perforation is elliptical in shape. From Fig. 5(b), it can be observed that the projectile does not penetrate the ceramic in the same straight path. Instead, the projectile turns away from the normal to the target as its oblique angle changes from an initial value of 30° to around 45° at rest. The projectile gets also eroded and blunted during the penetration process and its length is reduced to 6.9 mm (2.4 mm of which is the eroded length). The projectile erosion in oblique impact

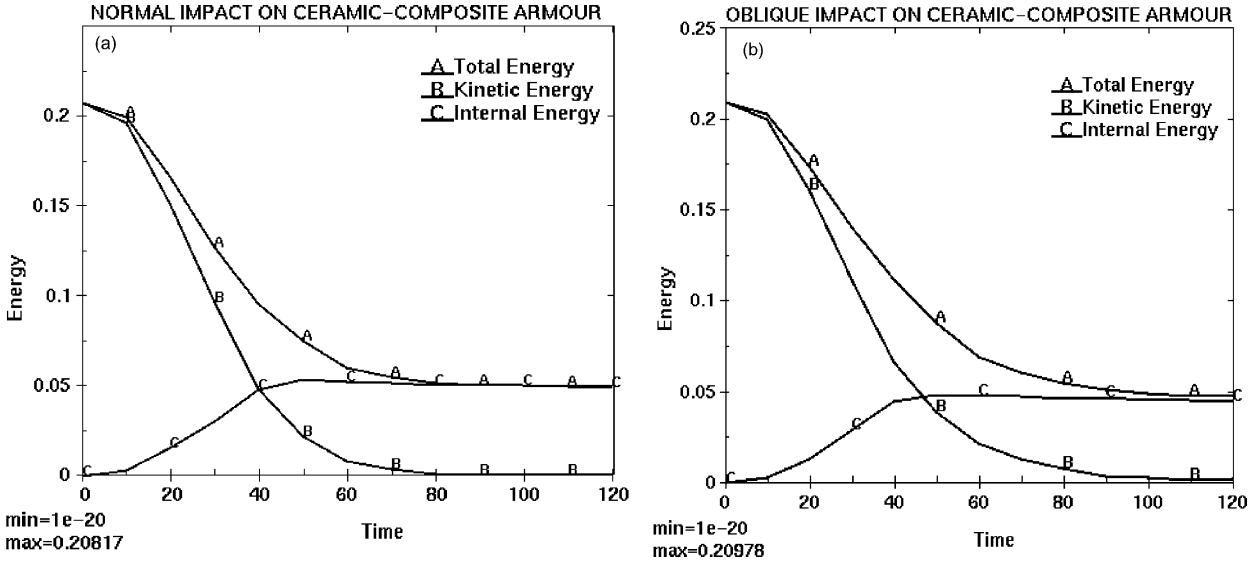

Fig. 4. Global energy (KJ) versus time (μs). (a) Normal impact and (b) oblique impact.

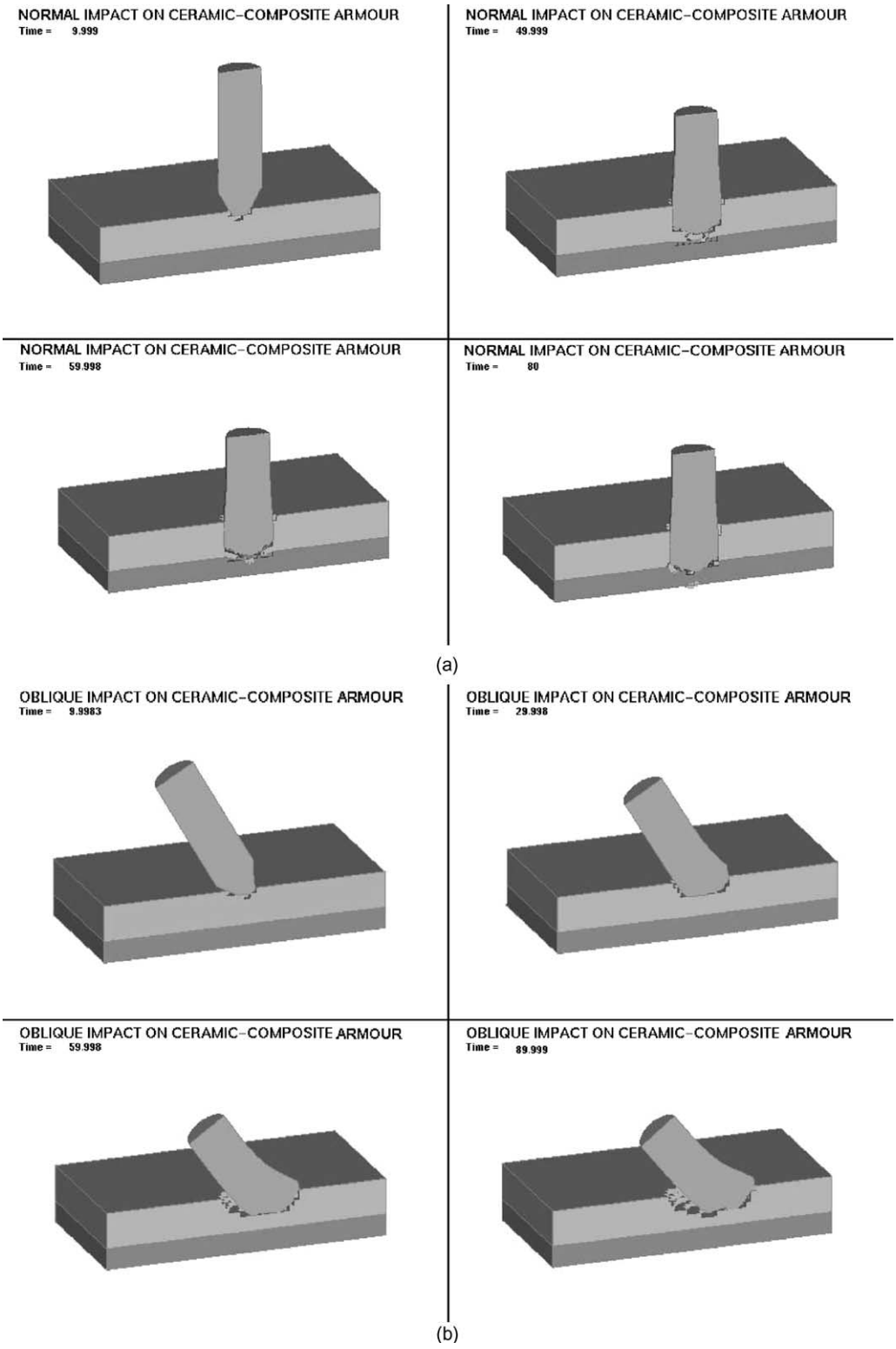

Fig. 5. Impact processes ($V = 315$ m/s). (a) Normal impact and (b) oblique impact.

is greater than that in normal impact because the penetration path in this case is longer than that in normal impact.

The distribution of effective stresses is shown in Fig. 6. The large stresses occur in front of the projectile and reduce in magnitude when the projectile is stopped.

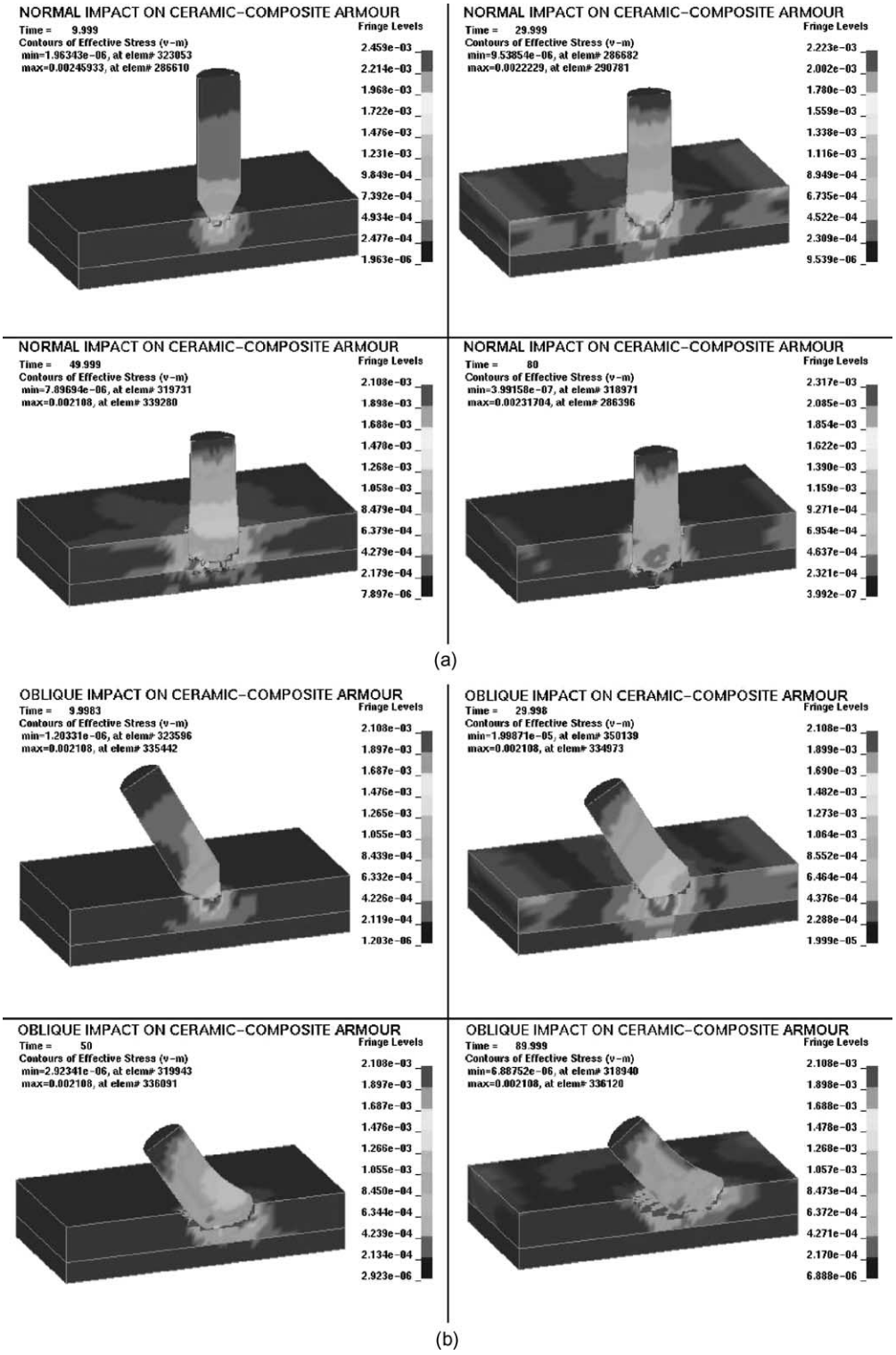

Fig. 6. Distribution of effective stresses (10^3 GPa). (a) Normal impact and (b) oblique impact.

The distribution of σ_x, σ_z, τ_{yz}, and τ_{zx} for the ceramic element 342 514, which is located at the ceramic–composite interface, 0.25 mm in the x-direction and 3.7 mm in the y-direction away from the centre, are shown in Fig. 7. It is seen that all of these stresses can be positive and negative at different stages. During impact, the interlaminar stresses σ_z, τ_{yz}, and τ_{zx} cause delamination between the ceramic and composite while the normal stress σ_x causes local bending and fibre fracture. That maximum σ_z for normal impact was found to be

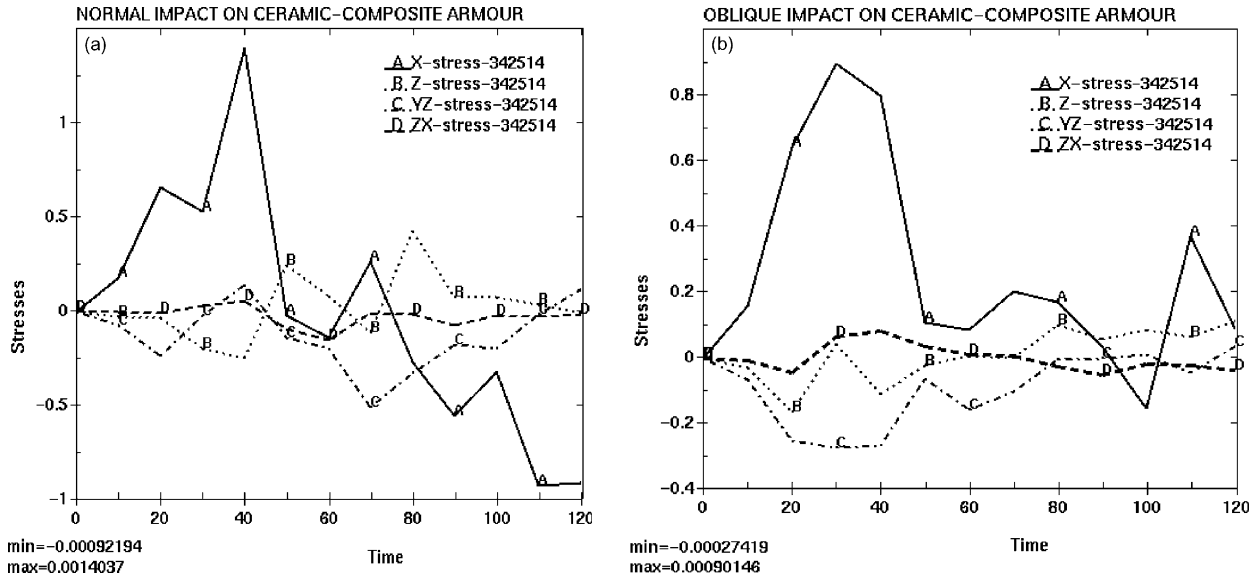

Fig. 7. σ_x, σ_z, τ_{yz}, τ_{zx} (GPa) versus time (μs) at ceramic–composite interface. (a) Normal impact and (b) oblique impact.

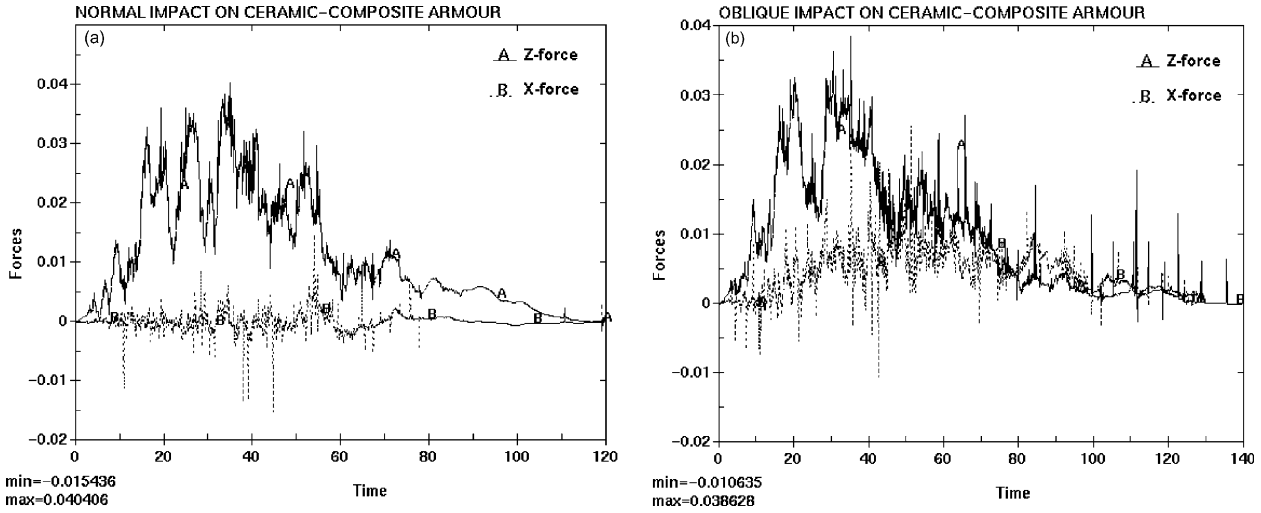

Fig. 8. X- and Z-force (10^3 KN) versus time (μs) at projectile–ceramic interface. (a) Normal impact and (b) oblique impact.

around 400 MPa. If the interface or the bonding between the ceramic and composite is not strong enough to withstand this tensile stress, delamination failure will take place. For both normal and oblique impacts, σ_x was found to be much greater than the other stresses. However, stresses for oblique impact, especially σ_z, τ_{yz}, and τ_{zx} are much lower than that for normal impact. So the possibility of delamination failure for oblique impact is much lower than that for normal impact.

Fig. 8 gives the distribution of the X-force and the Z-force at projectile–ceramic interface for normal impact (Fig. 8(a)) and oblique impact (Fig. 8(b)). For both the normal and oblique impacts, the Z-force is the most dominant, and it reaches the peak value at around 18 μs, albeit lasting a longer time for normal impact. For oblique impact, the X and Z forces have separate peak values. In particular, the X-force increases gradually until $t = 50$ μs, where it starts decreasing gradually from that point on.

4. Conclusion

Finite element models of the normal and oblique impacts of 7.62 AP round onto ceramic–composite armours were developed. Developed models had the ability to capture projectile erosion, ceramic conoid formation, as well as the failure of the ceramic and composite plates. The preliminary computations demonstrated reasonable correlation with existing experimental data, which allow us to conclude that the

numerical models can be used for an improved design of lightweight armours.

The various numerical simulations presented the details of penetration processes, distributions of energy, stresses etc. of normal and oblique impact at a velocity of 315 m/s. In particular, it was found that the distributions of global kinetic, internal and total energy versus time are similar for normal and oblique impact. However, the interlaminar stresses at the ceramic–composite interface and the forces at the projectile-ceramic interface for oblique impact were found to be smaller than those for normal impact. Furthermore, it was found that when a projectile impacts obliquely on the armour, it changes its angle during the perforation, forming an elliptical cavity at the tip of projectile. Finally, it was observed that the projectile erosion in oblique impact is slightly greater than that in normal impact.

Acknowledgements

The authors would like to gratefully acknowledge Materials and Manufacturing Ontario (MMO)'s financial support of this research project.

References

[1] Wilkins ML, et al. Fourth progress report of light armour program. Report UCRL 50694, Lawrence Radiation Laboratory, University of California, 1969.
[2] Cortes R et al. Numerical modeling of normal impact on ceramic composite armours. Int J Impac Eng 1992;12(4):639–51.
[3] Wang B, Lu G, Lim MK. Experimental and numerical analysis of the response of aluminum oxide tiles to impact loading. J Mater Process Technol 1995;51:321–45.
[4] Wilkins ML, et al. Fourth progress report of light armour program. Report UCRL 50694, Lawrence Radiation Laboratory, University of California, 1969.
[5] Espinosa HD et al. A numerical investigation of penetration in multilayered material/structure system. Int J Solids Struct 1997;35:2975–3001.
[6] Zaera R et al. Modelling of the adhesive layer in mixed ceramic/metal armour subjected to impact. Composites: Part A 2000;31:823–33.
[7] Lee M, Yoo YH. Analysis of ceramic/metal armour systems. Int J Impact Eng 2001;25:819–29.
[8] Arndt SM, Coltman JW. Design trade-offs for ceramic/composite armor materials. Proc 22nd Int SAMPE Technical Conf 1990;6–8:278–92.
[9] Chocron Benloulo IS, Sanchez-Galvez V. A new analytical model to simulate impact onto ceramic/composite armors. Int J Impact Eng 1998;21(6):461–71.
[10] Sanchez Galve V, Galvez Diaz-Rubio F. Ballistic impact on ceramic/composite armours. In: Jones N et al., editors. Structures under shock and impact V. Computational Mechanics Publications; 1998. p. 673–81.
[11] Cortes R et al. Numerical modeling of normal impact on ceramic composite armours. Int J Impact Eng 1992;12(4):639–51.
[12] Hetherington JG, Lemieux PF. The effect of obliquity on the ballistic performance of two component composite armours. Int J Impact Eng 1994;15:133–7.
[13] Sadanandan S, Hetherington JG. Characterisation of ceramic/steel and ceramic/aluminium armours subjected to oblique impact. Int J Impact Eng 1997;19:811–9.
[14] Zaera R, Sanchez-Galvez V. Analytical modelling of normal and oblique ballistic impact on ceramic/metal lightweight armours. Int J Impact Eng 1998;21(3):133–48.
[15] Tata A. A theory for the deceleration of long rods after impact. J Mech Phys Solids 1967;15:387–99.
[16] Alekseevskii VP. Penetration of a rod into a target at high velocity. In: Combustion explosion and shock waves, vol. 2. New York, USA: Faraday Press; 1966.
[17] Woodward RL. A simple one-dimensional approach to modelling ceramic composite armour defect. Int J Impact Eng 1990;9(4):455–74.
[18] den Reijer PC. Impact on ceramic faced armours, Ph.D Thesis, Delft University of Technology, 1991.
[19] LS-DYNA Keyword user's manual version 960, Livermore Software Technology Corporation, March 2001.
[20] LS-DYNA Theoretical manual, Livermore Software Technology Corporation, May 1998.
[21] Hetherington JG. The optimization of two component composite armours. Int J Impact Eng 1992;12:409–14.
[22] Mayseless M et al. Impact on ceramic targets. J Appl Mech 1987;54:373–8.
[23] Sanchez-Galvez V. Impact behaviour of lightweight armours. In: Jones N, Brebbia CA, Watson AJ, editors. Structures under shock and impact IV. Computational Mechanics Publications; 1996.